Int. J. Electrochem. Sci., 11 **(2016)** 8972 – 8980, doi: 10.20964/2016.11.02

International Journal of
ELECTROCHEMICAL
SCIENCE
www.electrochemsci.org

Application of Single-Walled Carbon Nanohorn Modified Electrode for the Direct Electrochemistry of Myoglobin

Lijun Yan, Xueliang Niu, Zuorui Wen, Xiaoyan Li, Xiaobao Li, Wei Sun[*]

Key Laboratory of Tropical Medicinal Plant Chemistry of Ministry of Education, College of Chemistry and Chemical Engineering, Hainan Normal University, Haikou 571158, P. R. China
[*]E-mail: swyy26@hotmail.com

Received: 15 July 2016 / *Accepted:* 10 September 2016 / *Published:* 10 October 2016

An electrochemical biosensor was fabricated with myoglobin (Mb), single-walled carbon nanohorns (SWCNHs) and carbon ionic liquid electrode (CILE). By applying chitosan (CTS) film on the electrode surface, the modified electrode was constructed and demonstrated as CTS/Mb/SWCNHs/CILE. Spectroscopic data proved that Mb remained the secondary structure within mixture. Cyclic voltammogram of CTS/Mb/SWCNHs/CILE exhibited a pair of well-defined redox peaks, showing that direct electron transfer of Mb with CILE was realized due to the acceleration effect of SWCNHs. The bioelectrode displayed excellent electrocatalytic behaviors to the reduction of tricholoacetric acid and $NaNO_2$.

Keywords: Direct electrochemistry. electrocatalysis. single-walled carbon nanohorns. myoglobin. carbon ionic liquid electrode

1. INTRODUCTION

Direct electron transfer (DET) of redox proteins/enzymes with electrode is of great importance in bioelectrochemistry [1]. The investigation can be used to explore the electron transfer mechanism in biological system and the results can be applied to the preparation of various bioelectronics devices [2]. In general it is different for the proteins to transfer electrons to the electrode due to the deeply buried electroactive center inside the proteins. The diffusional efficient of the proteins is slow with the denaturation on the electrode interface. To solve this challenge modified electrodes and suitable immobilization methods are designed to accelerate the direct electrochemical reaction [3, 4].

Single-walled carbon nanohorns (SWCNHs) is a novel carbon nanomaterial that has aroused much attentions, which exhibited the characteristics including excellent porosity, large surface area,

mechanical electronic properties, high purity with low toxicity [5]. Different synthesis methods of SWCNHs have been devised, which has the applications in the construction of microelectrical devices and electrochemical biosensors [6]. The high conductivity of $SWCNH_S$ is benefit for the electrons conducting for the biomolecules and the large surface is favorable for the increase of the loading amount of the target analytes on its surface. Therefore SWCNHs based electrochemical sensor has been exhibited higher sensitivity with many applications. Dai et al. detected 4-aminophenylarsonic acid with ionic liquid and carbon nanohorns modified glassy carbon electrode (GCE) [7]. Lv et al. fabricated aptamer-based SWCNHs sensors for ochratoxin A detection [8]. Zhu et al. investigated the electrochemical behaviors and voltammetric detection of two amino acids with SWCNHs/GCE [9]. Zhao et al. studied nanogold-enriched carbon nanohorn as label for electrochemical investigations of biomarker with a disposable immunosensor [10].

In this paper SWCNHs modified electrode was prepared for the direct electrochemistry of myoglobin (Mb). Carbon ionic liquid electrode (CILE) is selected as the substrate working electrode, which has been proven to have high electrical conductivity, wide electrochemical window, low background current, strong response signal and good stability [11-15]. Then Mb and SWCNHs modified CILE was got and chitosan (CTS) film was applied to fix them on the electrode surface. The modifiers on the electrode could form a suitable microenvironment to retain the microstructure and the activity of the immobilized Mb. The as-prepared Mb based bioelectrode was used to study the electrocatalytic activity to the reduction of tricholoacetric acid (TCA) and $NaNO_2$.

2. EXPERIMENTAL PART

2.1. Reagents

SWCNHs (Nanjing XFNANO Materials Tech. Ltd. Co., China), Mb (MW 17800, Sigma-Aldrich Co., USA), 1-hexylpyridinium hexafluorophosphate ($HPPF_6$, Lanzhou Yulu Fine Chem. Ltd. Co., China), graphite powder (partied size of 30 μm, Shanghai Colloid Chem. Co., China) and chitosan (Xiya Chem. Ltd. Co., China) were used. 0.1 mol L^{-1} phosphate buffer solution (PBS) were employed as the supporting electrolyte. The reagents used were of analytical grade with doubly redistilled water to prepare solutions.

2.2. Apparatus

All the cyclic voltammograms were recorded on a CHI 1210A electrochemical workstation and electrochemical impedance spectroscopy (EIS) on CHI 660D electrochemical workstation (Shanghai Chenghua Instrument, China) with a three electrode system, which was consisted of a platinum auxiliary electrode, a saturated calomel reference electrode and a modified CILE working electrode. Fourier transform infrared (FT-IR) spectroscopic experiment was operated on Nicolet 6700 FI-IR spectrometer (Thermo Fisher Scientific Inc., USA). Scanning electron microscopy (SEM) was performed on a JSM-7100F (Japan Electron Company, Japan) with an accelerating voltage of 5 kV.

2.3. Preparation of the Mb modified electrode

CILE was made with $HPPF_6$ as the binder [16], which was polished to a mirror-like surface on weighing paper. SWCNHs modified CILE was got by covering 6.0 μL of 1.0 $mg \cdot mL^{-1}$ SWCNHs solution on bare CILE. Then 6.0 μL of 15 $mg \cdot mL^{-1}$ Mb and 8 μL of 0.5 $mg \cdot mL^{-1}$ CTS (in 0.5% HAC) were dropping onto SWCNHs/CILE in sequence. After dried in the air the modified electrode was named as CTS/Mb/SWCNHs/CILE. Other electrodes including CTS/Mb/CILE, CTS/CILE etc. were made and used for the comparison of electrochemical behaviors.

3. RESULTS AND DISCUSSION

3.1. SEM images of SWCNHs modified electrode

Fig. 1 A and B displayed the SEM images of SWCNHs on the electrode surface with different magnitude, which gave the typical horn-shaped sheath of SWCNHs with the partly aggregation and a porous structure was formed with average radius of 80 to 100 nm. After Mb was casted on SWCNH, an obvious film could be found in Fig.1 C.

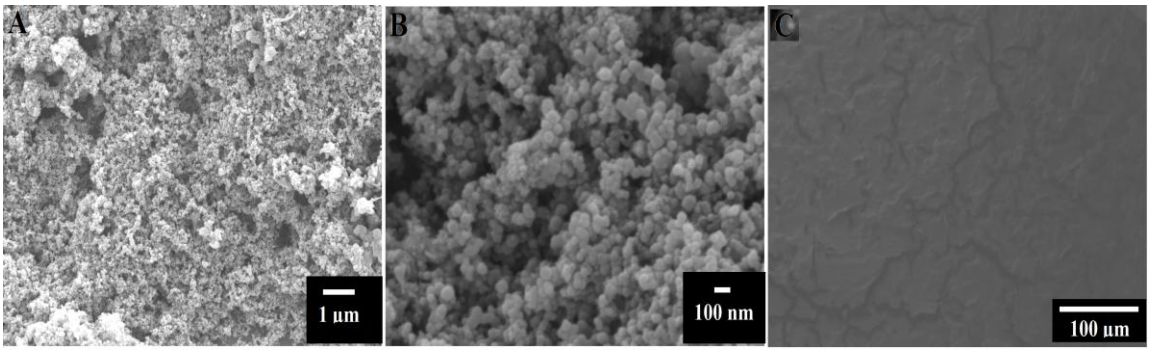

Figure 1. SEM images of SWCNHs/CILE with different magnitude (A), (B);(C) Mb/SWCNHs/CILE.

3.2 Spectroscopic results

The conformational integrity of Mb molecules was checked by FT-IR spectroscopy. The data of the secondary structure of polypeptide chain can be proved by the groups of amide I (1700-1600 cm^{-1}) and amide II (1620-1500 cm^{-1}) bands of redox proteins [17]. As shown in Fig. 2a, the amide I and II of Mb were got at 1647.7 cm^{-1} and 1547.8 cm^{-1}. The mixture of Mb within SWCNHs had the values of 1648.2 cm^{-1} and 1532.5 cm^{-1} (Fig. 2b). Therefore Mb mixed with SWCNHs retained its native structure without any changes, and SWCNHs exhibited good biocompatibility and did not influence the structure of Mb after mixing.

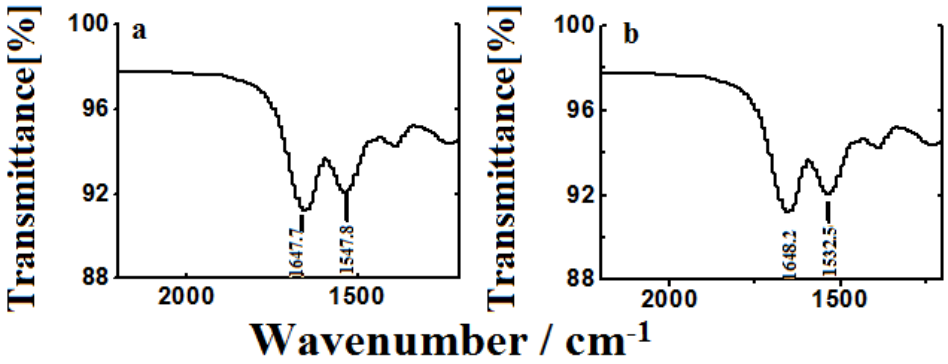

Figure 2. FT-IR spectra of (a) Mb and (b) Mb-SWCNHs mixture.

3.3 Electrochemical characteristics of the modified electrodes

The impedance changes of modified electrodes can be checked by EIS and the semicircle diameter of EIS can represent for the electron transfer resistance (Ret), which reflects the electron transfer kinetics of redox-probe on the electrode surface [18]. As shown in Fig. 3A, EIS of CILE (20.03 Ω, curve a), CTS/CILE (34.28 Ω, curve b) and CTS/Mb/CILE (49.22 Ω, curve c) were got respectively. The gradually increase of the Ret values were due to the presence of CTS film and Mb that obstructed the electron transfer of probe. The Ret values of CTS/Mb/SWCNHs/CILE and CTS/SWCNHs/CILE decreased to 12.5 Ω (curve d) and 7.9 Ω (curve e), implying the interfacial resistance was small. SWCNHs are good conductive carbon material that can be easier for the electron transfer. SWCNHs exhibited excellent electrochemical conductivity on the modified electrode with other specific characteristics including high surface area, optical transparency, good biocompatibility [18].

Electrochemical evaluation of different electrodes was performd by cyclic voltammetric technique with $K_3[Fe(CN)_6]$ as redox probe. Cyclic voltammograms of different electrodes were present in Fig. 3B. The redox currents of CILE (curve c), CTS/CILE (curve b) and CTS/Mb/CILE (curve a) were decreased in turn, indicating that CTS and Mb blocked the electron transfer of $K_3[Fe(CN)_6]$. The electrochemical response of CTS/Mb/SWCNHs/CILE (curve d) increased greatly with the peak current as 3.96 times higher than that of CTS/Mb/CILE (curve a), and the response of CTS/SWCNHs/CILE (curve e) was the biggest, which was ascribed to the excellent electrical conductivity of SWCNHs. In addition the effective surface area (A) was determined using Randles-Servick equation ($Ip=2.69\times10^5 n^{3/2} A\, D^{1/2} C^* \upsilon^{1/2}$) by changing scan rate [19], where Ip, A, n, C*, D and υ are the peak current, effective surface area, electron transfer number, concentration of $K_3[Fe(CN)_6]$, diffusional coefficient of $K_3[Fe(CN)_6]$ and scan rate, respectively. For $K_3[Fe(CN)_6]$ solution (n=1, $D=7.6\times10^{-6}$ cm^2 s^{-1}), the effective surface area of CILE and SWCNHs/CILE could be calculated as 0.213 and 0.418 cm^2, indicating SWCNHs could effectively increase the interfacial area.

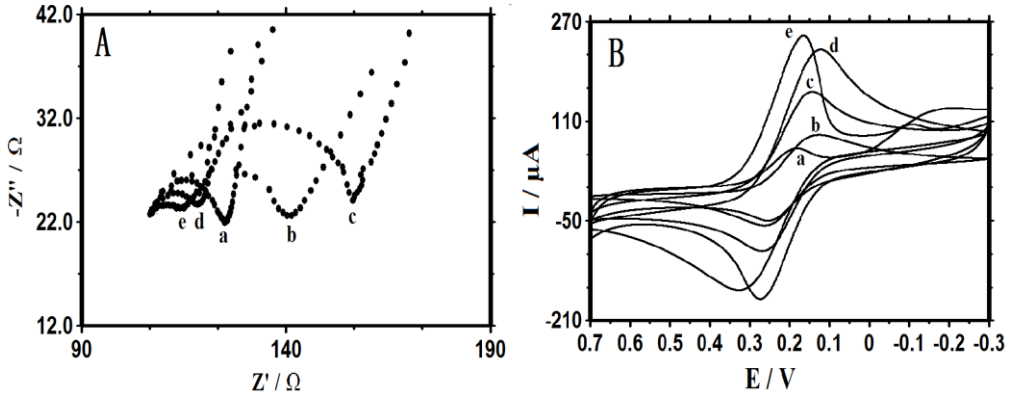

Figure 3. (A) EIS of (a) CILE; (b) CTS/CILE; (c) CTS/Mb/CILE; (d) CTS/Mb/SWCNHs/CILE; (e) CTS/SWCNHs/CILE in a 10.0 mmol L^{-1} $K_3[Fe(CN)_6]$ and 0.1 mol L^{-1} KCl mixture solution with the frequencies ranging from 10^5 to 10^{-1} Hz; (B) Cyclic voltammograms of different electrodes in a 1.0 mmol L^{-1} $K_3[Fe(CN)_6]$ and 0.5 mol L^{-1} KCl mixture solution with scan rate as 100 mV s^{-1}. Electrodes: (a) CTS/Mb/CILE, (b) CTS/CILE, (c) CILE, (d) CTS/Mb/SWCNHs/CILE and (e) CTS/SWCNHs/CILE.

3.4 Direct electrochemical behavior of the Mb modified electrode

As shown in Fig. 4, cyclic voltammetric technique was performed to check the voltammetric behaviors of modified electrodes in 0.1 mol L^{-1} PBS (pH 3.0). No peak can be observed on three kinds of electrodes (CILE curve a, CTS/CILE curve b, CTS/SWCNHs/CILE curve c), suggesting that there is no redox reaction occurred. However, a pair of unsymmetrical redox peaks was monitored on CTS/Mb/CILE (d), which indicated that slow electron transfer was occurred between Mb and CILE. Electrochemical response of CTS/Mb/SWCNHs/CILE (e) was enhanced with a pair of well-defined redox peaks (Epc as -0.285 and Epa as -0.190 V), and the value of redox peak currents increased to 1.5 times higher than that of CTS/Mb/CILE. Multi-scan cycling voltammetric results indicated that the redox peaks remained constant. The separation of peak potentials (ΔEp) was calculated as 95 mV and the formal peak potential ($E^{0\prime}$) was -0.237 V (vs. SCE), which was the typical characteristic of electroactive heme Fe(III)/Fe(II) redox couples.

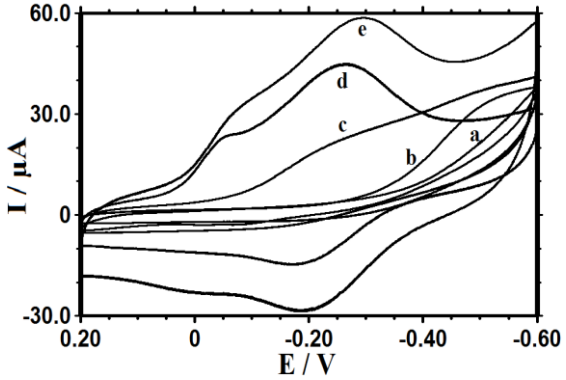

Figure 4. Cyclic voltammongrams of different modified electrodes in pH 3.0 PBS with scan rate as 100 mV s^{-1}. Electrodes (from a to e): CILE, CTS/CILE, CTS/SWCNHs/CILE, CTS/Mb/CILE, CTS/Mb/SWCNHs/CILE.

To further investigate the electrochemical behaviors of Mb on SWCNHs/CILE, the effect of scan rate was studied with the data listed in Fig. 5A. When scan rate increased from 0.05 to 0.95 V s^{-1}, the redox peaks currents were proportional to scan rate, indicating Mb on the electrode had a typical surface-controlled electrochemical process. From Fig. 5B the linear regression equations were expressed as Ipc (μA) = 149.80 υ (V s^{-1}) - 10.79 (γ = 0.992) and Ipa (μA) = -128.61 υ (V s^{-1}) + 9.39 (γ = 0.994). Also the peak potential (Ep) linearly increased with lnυ, and the linear regression equations were Epc (V) = -0.053 lnυ (V s^{-1})-0.197 (γ = 0.997) and Epa (V) = 0.042 lnυ (V s^{-1}) - 0.133 (γ = 0.998) (Fig. 5C). The electron transfer rate constants (k_s) and electron transfer coefficient (α) could be estimated according to Laviron's method [20] with the values of 0.59 s^{-1} and 0.56, which indicated that SWCNHs provided a suitable microenvironment for Mb to undergo facile electron transfer reaction. By integration of the reduction peaks and using the equation (Q = nFAΓ*) [21], the surface coverage (Γ*) was 3.00×10^{-9} mol cm^{-2}, which was lower than 1.72×10^{-8} mol cm^{-2} (the total amounts of Mb on the electrode surface). Therefore the fraction of electrochemical active Mb was 17.44 % of the total Mb on CILE surface.

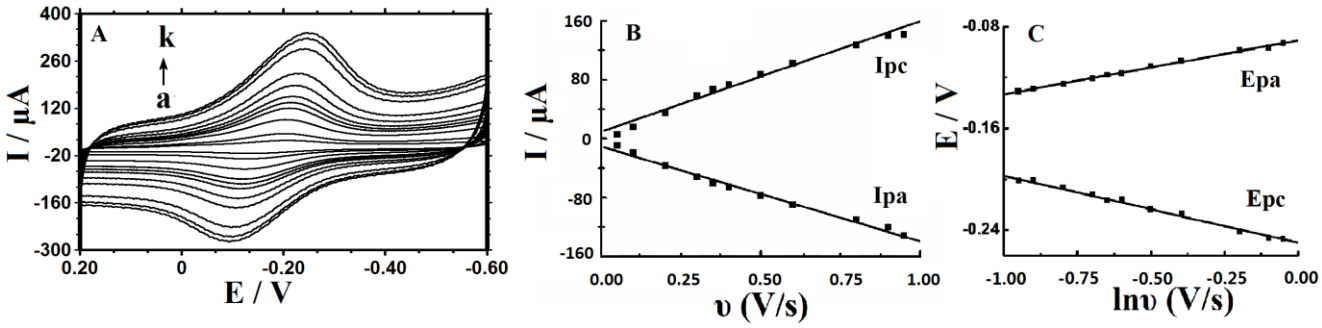

Figure 5. (A) Effect of scan rate (from a to k 50, 100, 200, 300, 350, 400, 500, 600, 800, 900, 950 mV s^{-1}) on redox peaks of CTS/Mb/SWCNHs/CILE in pH 3.0 PBS; (B) Linear relationship of redox peak currents versus scan rate (υ); (C) Liner relationship of the redox peak potential versus lnυ.

The effect of buffer pH on the redox reaction of Mb was studied within the pH range 3.0-7.0. The redox peak potentials shifted to the negative direction with the increase of solution pH value, indicating that protons participated in the electrochemical reaction. The linear regression between $E^{0\prime}$ and pH was got as $E^{0\prime}$ (mV) = - 51.72 pH - 12.83 (n = 5, γ = 0.988). The slope of -51.72 mV pH^{-1} approached to the theoretical data (-59.0 mV pH^{-1}), implying that the number of electrons transferred and hydrogen ions taking part in the electrode process was same [22]. Thus the whole electrode reaction were expressed as the following equation: Mb heme Fe (III) + H+ + e- ↔ Mb heme Fe (II).

3.5 Electrocatalytic activity of the Mb modified electrode

Mb had the electrocatalytical ability to reduce TCA and $NaNO_2$ due to its mimic peroxidase activity, which had been reported previously [23]. In order to check the activity of Mb at SWCNHs modified electrode, electro-reduction of TCA and $NaNO_2$ on CTS/Mb/SWCNHs/CILE were studied and the voltammograms were shown in Fig. 6. As for TCA the continuous addition resulted in the

disappearance of the oxidation peak with the simultaneous increase of a reduction peak at -0.223 V (Fig. 6A). While a new reduction peak was observed at -0.496 V with further increase of TCA concentration, which could be attributed to the formation of a highly reduced form of Mb [Mb Fe(I)] that might dechlorinate di- and mono-chloroacetic acid after the dechlorination of TCA with Mb Fe(II) [24]. A good linear relationship was established between the catalytic reduction peak current and the TCA concentration in the range from 0.9 to 51.0 mmol L^{-1} with the equation as Ipc (μA) = 2.635 C (mmol L^{-1}) + 8.19 (γ = 0.989). A detection limit (3σ) value for TCA was got as 0.3 mmol L^{-1}, which was lower than some reported values such as 0.5 mmol L^{-1} [25, 26], 0.613 mmol L^{-1} [27], 0344 mmol L^{-1} [28]. The current value exhibited a saturation value when TCA concentration was bigger than 51.0 mmol L^{-1}, indicating the electrocatalysis obeyed the Michaelis-Menten kinetic process. According to Lineweaver-Burk equation: $1/Iss = (1/Imax)(1+K_M^{app}/C)$ [29], where Iss, C and Imax are represent of the steady current after the addition of substrate, the bulk concentration of the substrate and the maximum current measured under the saturated substrate condition. Then K_M^{app} value was got as 43.16 mmol L^{-1}, which was smaller than that of 90.8 mmol L^{-1} [30] and 47.0 mmol L^{-1} [31]. Fig. 6B showed that the decrease of the anodic peak current with the reduction peak increased gradually at -0.703 V after continuous increase of $NaNO_2$ concentration. A good linear relationship was got between the catalytic reduction peak current and the $NaNO_2$ concentration in the range from 0.04 to 0.74 mmol L^{-1}, and the linear regression equation was Ipc (μA) = 91.994 C (mmol L^{-1}) + 3.058 (γ = 0.998). The detection limit for $NaNO_2$ was 0.13 mmol L^{-1} (3σ), which was smaller than some reported values such as 0.26 [32], 1.3 mmol L^{-1} [33] and 4.0 mmol L^{-1} [34]. The current exhibited a saturation value when $NaNO_2$ concentration was bigger than 0.74 mmol L^{-1}. Therefore the K_M^{app} for the electrocatalysis of $NaNO_2$ was got as 0.325 mmol L^{-1}, which was smaller than 3.66 mmol L^{-1} [32] and 27.6 mmol L^{-1} [33]. The lower K_M^{app} value indicated Mb in CTS/SWCNHs/CILE kept its bioactivity with excellent affinity to TCA and $NaNO_2$.

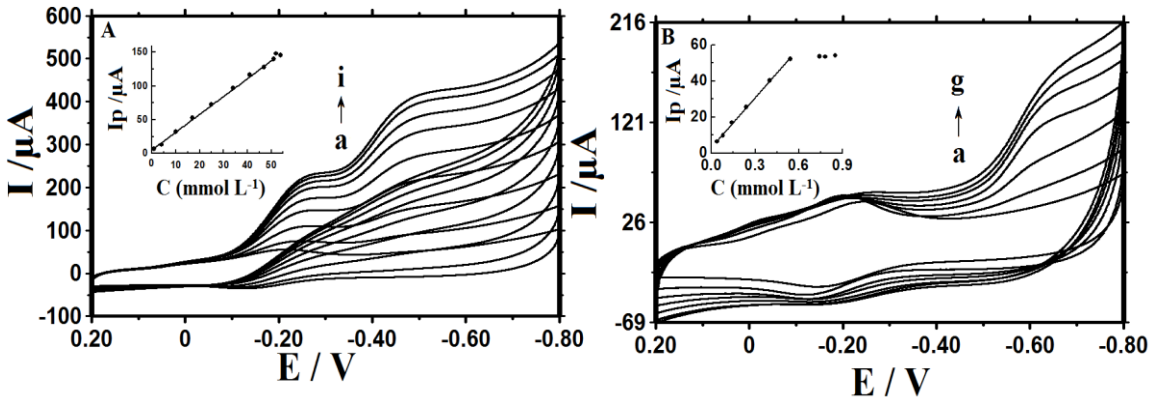

Figure 6. (A) Cyclic voltammogram of CTS/Mb/SWCNHs/CILE with different TCA concentration (a-i: 0.9, 4, 10, 17, 25, 34, 41, 47, 51 mmol L^{-1}) at scan rate of 100 mV s^{-1}. Inset was the linear relationship of catalytic reduction peak currents versus the TCA concentration; (B) Cyclic voltammogram of CTS/Mb/SWCNHs/CILE with different $NaNO_2$ concentration (a-g: 0, 0.04, 0.14, 0.34, 0.54, 0.74, 0.78 mmol L^{-1}) at scan rate of 100 mV s^{-1}. Inset was linear relationship of catalytic reduction peak currents versus the $NaNO_2$ concentration.

3.6 Sample detection

The proposed method was applied to TCA detection in tap water sample and standard addition method was used to verify the real application. In table 1 it can be seen that no TCA was detected in the water solution with the recovery in the range from 97.0 to 108.5 %. Therefore this Mb modified electrode could be applied to TCA content detection in water sample.

Table 1. Detection results of TCA in the tap water sample (n=3)

Sample	Detected ($mmol\ L^{-1}$)	Added ($mmol\ L^{-1}$)	Found ($mmol\ L^{-1}$)	Recovery (%)	RSD (%)
water	0	2.00	1.94	97.0	1.89
		4.00	4.22	105.5	2.95
		6.00	6.51	108.5	3.32

4. CONCLUSION

In this paper, the electroactivity of Mb and SWCNHs modified electrodes were investigated by different electrochemical technique. SWCNHs exhibited the properties including high conductivity, large surface area with biocompatibility. Spectroscopic test indicated that Mb retained its native structure with SWCNHs. Obvious redox peaks from direct electron transfer of Mb appeared on CTS/Mb/SWCNHs/CILE, which indicated that direct electrochemistry of Mb with the modified electrode was realized. By using CTS/Mb/SWCNHs/CILE as the working electrode, a novel third-generation electrochemical sensor was established and further employed for the electrocatalytic detection of TCA and $NaNO_2$ with high sensitivity and good reproducibility.

ACKNOWLEDGEMENTS
We acknowledge the financial support from National Natural Science Foundation of China (Nos. 21166009, 81160391), International S&T Cooperation Program of China (2014DFA40850), the International S&T Cooperation Project of Hainan Province (KJHZ2015-13), the Natural Science Foundation of Hainan Province (20162031) and Graduate Student Innovation Research Project of Hainan Province (Hys2016-61).

References

1. S. Iijima, M. Yudasaka, R. Yamada, S. Bandow, K. Suenaga, F. Kokai and K. Takahashi, *Chem. Phys. Lett.* 309 (1999) 165.
2. A. Thess, R. Lee, P. Nikolaev, H. Dai, P. Petit, J, Robert and C.H. Xu, *Science* 273 (1996) 483.

3. L.C. Qin and S. Iijima, *Chem. Phys. Lett.* 269 (1997) 65.
4. S. Ustsumi, K. Uvita and H. Kanoh, *J. Phys. Chem. B* 110 (2006) 7165.
5. S. Yoshida and M. Sano, *Chem. Phys. Lett.* 433 (2006) 97.
6. R. Yuge, T. Ichihashi and Y. Shimakawa, *Adv. Mater.* 16 (2004) 1420.
7. H. Dai, L.S. Gong, S.Y. Lu, Q.R. Zhang, Y.L. Li, S.P. Zhang, G.F. Xu, X.H. Li, Y.Y. Lin and G.N. Chen, *Microchim. Acta* DOI 10.1007/s00604-015-1445-4.
8. L. Lv, C.B. Cui, C.Y. Liang, W.R. Quan, S.H. Wang and Z.J. Guo, *Food Control* 60 (2016) 296.
9. S.Y. Zhu, J. Zhang, X.E. Zhao, H. Wang, G.B. Xu and J.M. You, *Microchim. Acta* 181 (2014) 445.
10. C.R. Zhao, D.J. Lin, J. Wu, L. Ding, H.X. Ju and F. Yan, *Electroanalysis* 25 (2013) 1044.
11. C.H. Bu, X.H. Liu and Y.J. Zhang, *Collids Surf., B* 88 (2011) 292.
12. R.T. Kachoosangi, M.M. Musameh and I. Abu-Yousef, *Anal. Chem.* 81 (2009) 435.
13. M.C. Buzzeo, R. G. Evans and R.G. Compton, *Chem. Phys. Chem.* 5 (2004) 1106.
14. F.Endres, *Chem. Phys. Chem.* 3 (2002) 144-154.
15. H. Sun, *J. Porous Mater*. 13 (2006) 393-397.
16. L.J. Yan, X.L. Niu, W.C. Wang, B.X. Li, X.H. Sun, C.J. Zheng, J.W. Wang and W. Sun, *Int. J. Electrochem. Sci.* 11 (2016) 1738.
17. L.J. Yan, W.C. Wang, B.X. Lei, J.W. Xi, P. Li, L. Liu, X. Zhang and W. Sun,; *Sensor Letters*, 11 (2016) 39.
18. X.Q. Liu, L.H. Shi, W.X. Niu, H.J. Li and G.B. Xu, *Biosens. Bioelectron.* 23 (2008) 1887.
19. A.J. Bard and L.R. Faulkner, Wiley, New York, 2001.
20. E. Laviron, *J. Electroanal. Chem.* 52 (1974) 355.
21. J. Wang, 3rd Ed. Wiley-VCH, New York, 2006.
22. I. Yamazaki, T. Araiso, Y. Hayashi, Y. Yamada and R. Makino, *Adv. Biophys.* 11 (1978) 249.
23. L. Shi, X. Liu and W. Niu, *Biosens. Bioelectron.* 24 (2009) 1159.
24. C.H. Fan, Y. Zhuang, G.X. Li, J.Q. Zhu and D.X. Zhu, *Electroanalysis* 12 (2000) 1156.
25. X.F. Wang, Z. You, H.L. Sha, S.X. Gong, Q.J. Niu and W. Sun, *Microchim. Acta* 181 (2014) 767.
26. J. Lou, Y. Deng, Y.X. Lu, Y. Wang, C.X. Ruan and W. Sun, *Sensor Letters* 12 (2014) 1267.
27. C.X. Ruan, Z.L. Sun, J. Liu, J. Lou,W. Gao and W. Sun, Y.S. Xiao, *Microchim. Acta* 177 (2012) 457.
28. J. Lou, Lu, T.R. Zhan, Y.Q. Guo and W. Sun, *Ionics* 20 (2014) 1471.
29. W. Sun, D.D. Wang, R.F. Gao and K. Jiao, *Electrochem. Commun*. 9 (2007) 1159.
30. W. Sun, X.Q. Li and K. Jiao, Electroanalysis 21 (2009) 959.
31. W. Sun, Y. Wang, X.Q. Li, J. Wu, T.-R. Zhan and K. Jiao, *Electroanalysis* 21 (2009) 2454.
32. F. Shi, W.C. Wang, S.X. Gong, B.X. Lei, G.J. Li, X.M. Lin, Z.F. Sun and W. Sun, J. *Chin. Chem. Soc.* 62 (2015) 554.
33. T.R. Zhan, M.Y. Xi, Y. Wang, W. Sun and W. Hou, *J. Colloid Interface Sci.* 346 (2010) 188.
34. G. Maduraiveeran, P. Manivasakan and R. Ramaraj, *Int. J. Nanotechnol*. 8 (2011) 925.